Low-dimensional magnetic systems in nanopore arrays

Noelia Bajales[1], María S. Viqueira[2], Lucia Avalle[1] Silvia E. Urreta[2] and Paula G. Bercoff[1,2]

[1]Instituto de Física Enrique Gaviola. CONICET, Argentina.
[2]Facultad de Matemática, Astronomía y Física, Universidad Nacional de Córdoba. Argentina.

FeCo nanowires 20 nm diameter are synthesized by AC electrodeposition using AAO membranes as templates. The hysteresis and structural properties of the as deposited nanowire arrays are characterized. The orientation dependence of the coercive field measured in the array is compared with the predictions of a magnetization reversal model involving the nucleation and propagation of a transverse wall. The model is promissory because it predicts the experimental curve shape quite well.

Index Terms— alumina template, FeCo nanowires, hysteresis properties, shape anisotropy, magnetization mechanisms.

I. INTRODUCTION

IRON-COBALT alloys are interesting for high temperature applications because they have high Curie temperatures (above 1100 K) and also high spontaneous magnetization. Near the equiatomic composition, the polycrystalline alloys also show a large saturation magnetostriction, of about $\lambda_S = 63 \ 10^{-6}$ [1]. However, even in the disordered state a quite low coercivity is observed, mainly due to a small magneto-crystalline anisotropy energy K_1, which varies between $5 \ 10^5$ erg/cm^3 to $-3 \ 10^5$ erg/cm^3 when the Co content changes from 0 to 60 at. % [1].

The strategies for improving coercivity are based on the construction of a high effective anisotropy, with contributions from size, shape, texture and composition effects. Fe-Co nanowires produced by template assisted electrodeposition to obtain medium to large aspect ratios ($Ar = l/d$, with l and d the nanowire length and diameter, respectively) are good examples of a large effective anisotropy based on shape effects. For AC electrodeposited nanowires ($Ar=20$) in the as-deposited condition, a coercivity of 0.15 T and a squareness S ($S=J_R/J_S$, with J_R and J_S the remanent and the saturation polarizations, respectively) of 0.7 have been found [2]. In wire arrays processed applying the same technique, but with $Ar=375$, coercivity and squareness values of 0.25-0.27 T and 0.95 are obtained [3], [4]. The values achieved with single crystalline wires, processed by DC electrodeposition are generally higher [5].

The AC electrodeposition technique is known to produce polycrystalline wires, with grains of a few nanometer [3], evidenced by transmission electron microscopy (TEM) in the dark field condition. This fine-grained microstructure is explained [2] by considering that the AC electrodeposition is not a continuous growth process because Fe^{+2} and Co^{+2} ions deposit into the pores only during a half AC cycle.

The magnetization reversal process in arrays of nanowires has attracted much attention [6]-[12]. Depending on the wire dimensions and geometry, homogeneous and localized magnetization modes have been proposed, to predict the coercivity values. For FeCo nanowires produced by AC electrodeposition many authors coincide [2], [3], [12] in concluding that magnetization reversion proceeds by the nucleation and further expansion of a transversal domain wall, that is, a localized, nucleation controlled mechanism.

In this article we report our results concerning the orientation dependence of the coercive field measured in an array of polycrystalline nanowires with composition near Fe$_{50}$Co$_{50}$ and the predictions of a magnetization reversal model considering the nucleation and propagation of a transverse wall [13]-[16].

II. EXPERIMENTAL PROCEDURES

Porous anodic aluminum oxide (AAO) templates 20 nm in diameter and uniform length of about 1 µm were prepared by a two-step anodizing process, on high purity (99.995%) aluminum foils, in a 0.3 M oxalic acid solution at 3ºC, by applying a DC voltage of 20 V [17], [18]. Previous to the anodization process the foil was degreased in an acetone bath and electropolished in a mixture of sulfuric and phosphoric acid.

The electrodeposition of FeCo nanowires was carried out in an aqueous electrolytic bath containing Fe^{+2} and Co^{+2} ions prepared with CoSO$_4$·7H$_2$O 0.2 M, FeSO$_4$·7H$_2$O 0.2 M, 0.009 M ascorbic acid and of H$_3$BO$_4$ 0.5M, which was added to enhance conductivity. The pH value was adjusted to 5 by adding few drops of diluted H$_2$SO$_4$.

The electrodeposition nanowires of nominal composition Fe$_{50}$Co$_{50}$ was conducted at room temperature under a sinusoidal wave of 200 Hz and 16 V rms during a few minutes, using a two-electrode electrochemical cell where the AAO template serves as a working electrode and a graphite rod as the auxiliary electrode.

The resulting samples were characterized by scanning electron microscopy (SEM) in a FE SEM Sigma Zeiss microscope with an Oxford EDS system. SEM images and EDS analyses were used to determine the morphology and the actual composition of the resulting nanowires, respectively. For these measurements, the AAO template and the Al support were dissolved in an aqueous 1M Na (OH) solution, leaving the metallic nanowires exposed.

In order to characterize the hysteresis properties and the magnetization mechanism operating in these samples, the hysteresis loops were measured at different sample orientations with respect to the applied magnetic field between

$\theta=0°$ (with the magnetic field parallel to the long nanowire axis) and $\theta=90°$ (with magnetic field perpendicular to the nanowire length). The total magnetic moment has contributions from the Al support (paramagnetic), the alumina template (diamagnetic) and the wires filling the pores (ferromagnetic). The measurements were performed at room temperature in a Lakeshore 7300 vibrating simple magnetometer (VSM) with applied fields up to 1.5 T.

III. RESULTS AND DISCUSSION

Fig. 1a shows SEM images of the alumina template and Fig. 1b displays the FeCo nanowires after the partial dissolution of the alumina template in a solution of NaOH (bottom panel).

FIG. 1 HERE

Analyses of different images indicate that even when the pores in the membrane have a mean length of 1 μm, they are not completely filled with the metals, resulting in nanowires with an average length l=0.8 μm. On the contrary, nanowires diameters are rather uniform, with a mean value of d = 20 nm. The wires are polycrystalline. Their mean grain size (30±10) nm was roughly estimated using the Scherrer formula, with the FWHM of the unique (FeCo (110)) peak observed in the X-ray diffraction pattern (not shown), which also evidenced a strong preferred (110) orientation perpendicular to the template surface.

The actual chemical composition of the FeCo nanowires was obtained by averaging EDS data from 60 individual sampling areas, uniformly distributed over the sample surface. The resulting composition, $Fe_{55}Co_{45}$ is relatively close to the nominal value.

TABLE 1 HERE

Fig. 2 shows the room temperature hysteresis loops (reduced polarization J/J_S vs. applied magnetic field H) of FeCo nanowires, for different external field orientations from $\theta=0°$ to $\theta=90°$. As expected, due to the large aspect ratio of the wires (Ar=40), shape anisotropy effects are dominant. In fact, the shape anisotropy field associated to the present wire geometry is given by $\mu_0 H_{shape}^A = J_S \Delta N \cong 1.1$ T, higher than the magnetocrystalline anisotropy field of FeCo alloys (about 0.5 $\mu_0 H_{cryst}^A (\text{Co}) = 0.9\,\text{T}$). Here, J_S is the alloy spontaneous polarization (2.45 T [1]), N_z is the demagnetizing factor along the wire axis (0.0117) and $\Delta N = N_\perp - N_z = 0.48$ is the difference in demagnetizing factors for these two normal directions.

FIG. 2 HERE

The total polarization J in the hysteresis loops is well fitted by a paramagnetic component from the Al substrate, a diamagnetic one from the Al_2O_3 membrane and a dominant ferromagnetic contribution arising from FeCo wires.

In order explore the magnetization reversal mechanism in these ordered, metallic nanowire arrays, the ferromagnetic hysteresis parameters were determined as functions of the angle θ between the nanowire long axis and the applied magnetic field. The resulting coercivity values $\mu_0 H_C$, relative remanence $J_R(\theta)/J_R(0)$ and squareness $S(\theta)=J_R(\theta)/J_S(\theta)$ are depicted in Fig. 3a, b and c, respectively.

Localized demagnetization modes, normally caused by structural features, are common phenomena in real polycrystalline nanowires, being largely responsible for the observed hysteretic behavior [8].

Based on the original ideas of Stoner and Wohlfarth [13], Escrig et al. [14] propose an analytical model to describe the angular dependence of the critical field for magnetization switching by a mechanism of nucleation and further propagation of a transverse domain wall along the nanowire length. The critical nucleation field is given by:

$$H_n^T(\theta) = -\frac{2(K_D(\omega_T) + K_{ca})\sqrt{1 - t^2 + t^4}}{\mu_0 M_S^2(1 + t^2)} M_S, \qquad (1)$$

where $K_D(\omega_T) = \frac{1}{4}\mu_0 M_S^2 [1 - 3N_z(\omega_T)]$ is an effective shape anisotropy constant, ω_T is the domain wall width, K_{ca} is the crystalline anisotropy constant, $t=\tan(\theta)^{1/3}$, and N_z is the demagnetizing factor along the wire axis. Then, the coercive field results [14]:

$$H_c^T(\theta) = \begin{cases} \left|H_n^T(\theta)\right|.............................0 \le \theta \le \pi/4 \\ 2\left|H_n^T(\pi/4)\right| - \left|H_n^T(\theta)\right|...\pi/4 \le \theta \le \pi/2 \end{cases}. \qquad (2)$$

For the present composition $Fe_{55}Co_{45}$, the crystalline anisotropy constant is reported to be K_{ca}= -0.15 x 10^5 J/m^3 [1]. The transversal domain wall thickness $\omega_T = \pi\sqrt{\frac{A}{Kca}} = 10\,\text{nm}$ is estimated considering A = 1.5 x 10^{-11} J/m^3 and $N_z(\omega_T) = 0.5$. An empirical rule [19], valid in soft nanowires, is that the coercivity is about one third of the theoretical nucleation field. This phenomenon is often observed when theoretical predictions are compared with data obtained from real systems. Sample defects, high local demagnetizing stray fields and other inhomogeneities largely reduce the anisotropy energy in sites which may act as nucleation catalysts, greatly reducing the critical nucleation field.

FIG. 3 HERE

In these kind of ordered arrays, results also indicate [20] that there is a quite strong dipolar field when the saturating field is applied perpendicular to the wire axis, while the dipolar interaction with all the magnetic moments aligned parallel to the wire axis is very weak, and can be ignored. Then, the easy magnetization axis becomes determined by the competition of dipolar interactions and shape anisotropy. Then, dipolar interactions are likely to affect the loops shape and also the coercive field. These effects are embodied in the empirical parameter α, which may take values about 0.3-0.5.

The values predicted by Eq. 2 for the coercive field $\mu_0 H_C$, with $\alpha = 0.3$ [19], [21], are plotted in Fig. 3a together with the experimental results. The predicted curve reproduces well both the shape of the experimental curve and the measured coercivity values. Fig. 3b shows the reduced remanence as a function of the angle θ and the solid line corresponds to the model proposed in [15] for an hexagonal array of noninteracting, single-crystal Ni nanowires, which states that

$$J_R(\theta) = J_R(0) \left| \cos \theta \right|.$$

In this case, the model cannot explain the abrupt drop in the relative remanence near $\theta = 0$ mainly because demagnetizing interactions are not considered. The gradual reduction of the loop squareness is shown in Fig. 3c. These models need further elaboration to account for the remanence behavior and the α parameter value on the basis of the array/wire microstructure and interactions.

REFERENCES

[1] C. O'Handley, *"Modern Magnetic Materials. Principles and Applications"*. John Wiley & Sons. 1st Ed. New York, 2000. p. 323.
[2] D.H. Qin, L. Cao, Q.Y. Sun, Y. Huang, H.L. Li. "Fine magnetic properties obtained in FeCo alloy nanowire arrays". *Chemical Physics Letters 3*58, 484–488, June 2002.
[3] Qingfeng Zhan, Ziyu Chen, Desheng Xue, and Fashen Li. H. Kunkel, Xuezhi Zhou, R. Roshko, . G. Williams. "Structure and magnetic properties of Fe-Co nanowires in self-assembled arrays". *Phys. Rev. B* 66, 134436, October 2002.
[4] M. Almasi Kashi, A. Ramazani, F. Es'haghi, S.Ghanbari, A. S. Esmaeily. "Microstructures and magnetic properties of as-deposited and annealed Fe_xCo_{1-x} alloy nanowire arrays embedded in anodic alumina templates" *Physica B* 405, 2620–2624, March 2010.
[5] C.X. Cui, , B.L. Wang, W. Yang, J.B. Sun. Journal of Crystal Growth Volume 324, Issue 1, 1 June 2011, Pages 168–17. Effect of deposition voltage and Co2+ concentration on the texture and magnetic properties of Co nanowire arrays
[6] D. J. Sellmyer, M. Zheng, R. Skomski, *J. Phys.: Condens. Matter* 13, (2001) R433. "Magnetism of Fe, Co and Ni nanowires in self-assembled arrays"
[7] H. Zeng, R. Skomski, L. Menon, Y. Liu, S. Bandyopadhyay, D.J. Sellmyer, *Phys. Rev. B* 65 (2002) 134426. "Structure and magnetic properties of ferromagnetic nanowires in self-assembled arrays".
[8] R. Skomski, H. Zeng, M. Zheng, D.J. Sellmyer, *Phys. Rev. B* 62(2000) 3900. "Magnetic localization in transition-metal nanowires"
[9] R. Skomski, H. Zeng, D.J. Sellmyer, *J. Magn. Magn. Mater.* 249 (2002) 175. "Incoherent magnetization reversal in nanowires".
[10] T. G. Sorop, C. Untiedt, F. Luis, M. Kröll, M. Rasa, L.J. de Jongh, *Phys. Rev. B* 67 (2003) 014402. "Magnetization reversal of ferromagnetic nanowires studied by magnetic force microscopy".
[11] P.M. Paulus, F. Luis, M.M. Kröll, G. Schmid, L.J. de Jongh, *J. Magn. Magn. Mater.* 224 (2001) 180.
[12] .Jian-Hua Gao, Qing-Feng Zhan, Wei He, Da-Li Sun, Zhao-Hua Cheng, "Thermally activated magnetization reversal process of self-assembled $Fe_{55}Co_{45}$ nanowire arrays". *J. Magn. Magn. Mater.* 305, 365–371, February 2006.
[13] (E. C. Stoner and E. P. Wohlfarth, Philos. Trans. R. Soc. London, Ser. A 240, 599 1948).
[14] J. Escrig, J. Bachmann, J. Jing, M. Daub, D. Altbir,, and K. Nielsch, *Phys. Rev. B* **77**, 214421 (2008). "Crossover between two different magnetization reversal modes in arrays of iron oxide nanotubes".
[15] -R. Lavín, J. C. Denardin, J. Escrig, D. Altbir, A. Cortés, and H. Gómez. Angular dependence of magnetic properties in Ni nanowire arrays. *J. Appl. Phys.* 106, 103903 (2009).
[16] L. G. Vivas, J. Escrig, D. G. Trabada, G. A. Badini-Confalonier[1], M. Vázquez. Magnetic anisotropy in ordered textured Co nanowires. *Appl. Phys. Lett.* 100, 252405 (2012)
[17] B.-Y. Yoo, S.C. Hernandez, B. Koo, Y. Rheem and N.V. Myung Water Sci. & Technol. 55, (2007) 149. "Electrochemically fabricated zero-valent iron, iron-nickel, and iron-palladium nanowires for environmental remediation applications".
[18] H. Uchida, Y. Matsumura, H. Uchida, H. Kaneko, *J. Magn. Magn. Mater.* **239** 540. 2002. "Progress in thin films of giant magnetostrictive alloys".
[19] R. Skomski. Exact nucleation modes in arrays of magnetic particles. *J. of Appl. Phys.* 91, 10-15 (2002).
[20] Qing-Feng Zhan, Jian-Hua Gao, Ya-Qiong Liang, Na-Li Di, and Zhao-Hua Cheng. Dipolar interactions in arrays of iron nanowires studied by Mössbauer spectroscopy. *Phys.Rev. B* 72, 024428 (2005).
[21] H. Kronmuller, T. Schrefl. Basic magnetic properties of nanocrystalline particles and particles ensembles. *NATO ASI Series,* Volume 247, pp 127-143, (1993).

TABLE I
EDS IRON AND COBALT COMPOSITION OF FECO NANOWIRES

Element	Average wt. %	Average %
Fe	1.87(3)	55
Co	1.54(3)	45
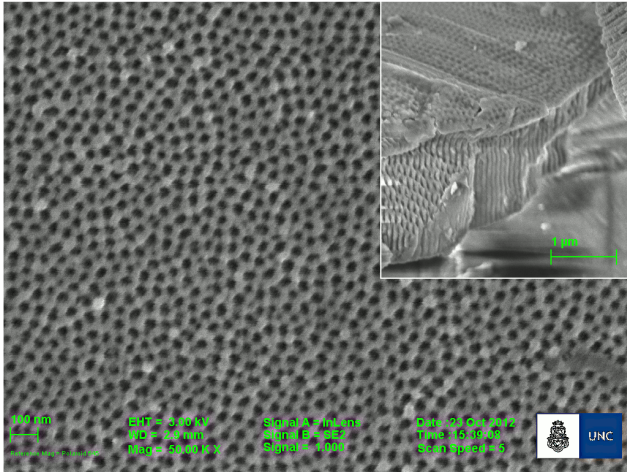
Fig. 1a. SEM micrograph showing a top view of the AAO template. The
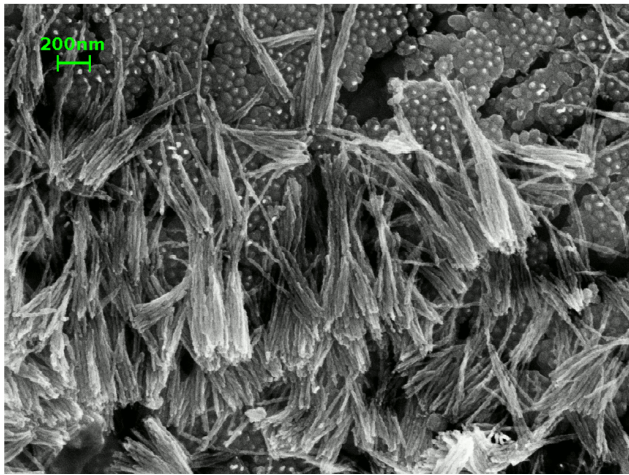
Fig. 1b. SEM micrograph showing the $Fe_{55}Co_{45}$ nanowires (diameter of ~20
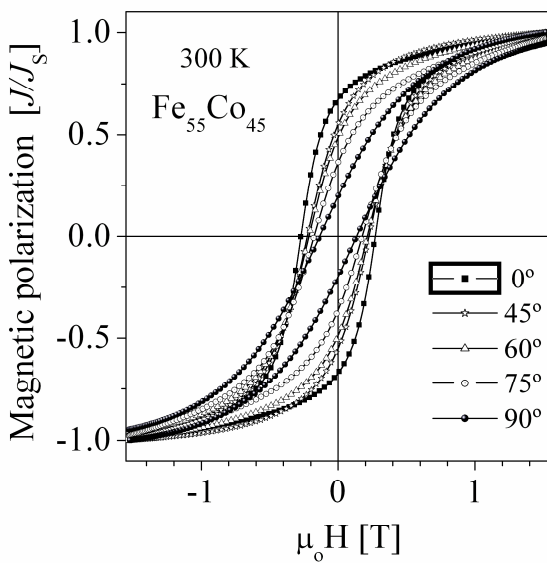
Fig. 2. Room temperature hysteresis loops of FeCo nanowires 0.8 µm long for different external field orientations from θ=0° to θ=90°.
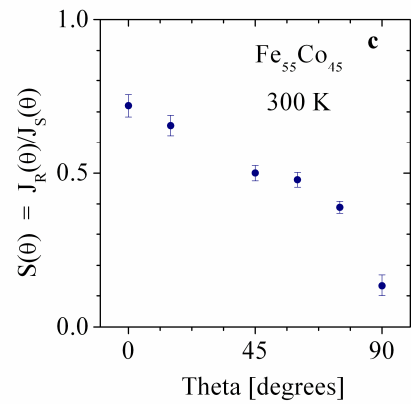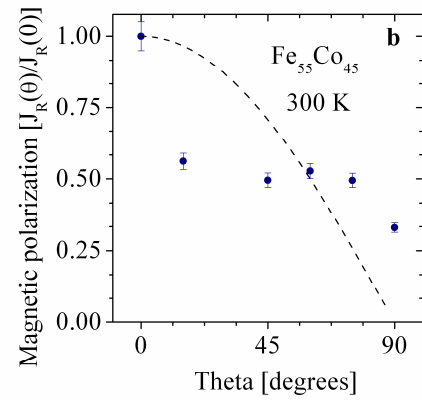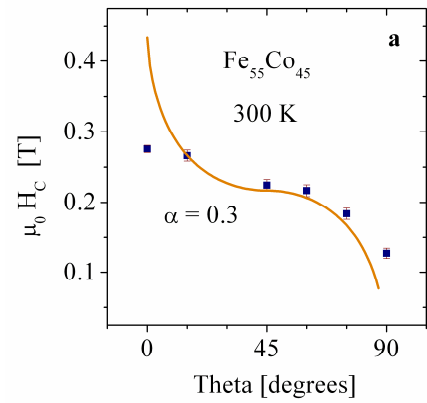
Fig. 3. Room temperature hysteresis parameters of a $Fe_{55}Co_{45}$ nanowire array as functions of the angle between the nanowire long axis and the applied field. (a) Coercivity $\mu_0 H_C$. The solid line corresponds to the theoretical prediction (Eq. 2) for magnetization reversal by transverse wall movement, using the factor α=0.3. (b) Relative remanence $J_R/J_R(0)$. The dashed line corresponds to the prediction from ref. [15], which is clearly not adequate for this system. (c) Squareness $S(\theta)=J_R(\theta)/J_S(\theta)$.